Journal of the European Ceramic Society 23 (2003) 1019–1026

www.elsevier.com/locate/jeurceramsoc

Process model of plasma enamelling

T. Zhang[a,*], Y. Bao[b], D.T. Gawne[b]

[a]*School of Engineering, Kingston University, London, UK*
[b]*School of Engineering, South Bank University, London, UK*

Received 15 March 2002; received in revised form 26 June 2002; accepted 30 June 2002

Abstract

A computational model has been developed to simulate the deposition of enamel on steel substrates by the use of plasma spraying. The model predicts the temperature profiles of the feedstock particles during their flight in the gas jet and the concurrent heating of the substrate. A process window is predicted for enamel deposition in terms of plasma gas composition and feedstock particle size. The model also predicts that the plasma jet produces a thermal shock at the surface of the coating and a high temperature gradient through its thickness during the scanning action. A series of experimental trials confirmed that plasma spraying could successfully produce dense coatings on steel. An inherent advantage of the process is that the enamel feedstock powder is fused separately in the plasma while the substrate remains at a low temperature. This enables enamelling to be carried out in a single stage operation without the need for a furnace, which offers the potential of widening the applicability of enamel coatings.

Keywords: Coatings; Enamel; Glass coatings; Plasma spraying; Thermal spraying

1. Introduction

In conventional vitreous enamelling, the enamel slurry or powder is applied to a component and both are heated one or more times in a furnace to approximately 850 °C. This temperature is necessary in order to fuse the enamel to the steel but is a source of difficulty in both processing and product quality. Specifically, the need for the furnace treatment limits the size of the component to the furnace dimensions and eliminates the possibility of on-site enamelling. The repair of damaged or defective enamelled articles also cannot be carried out on-site satisfactorily and complete re-processing is normally required. As regards the product, besides the risk of softening and distortion of the steel substrate, hydrogen may be evolved from the steel causing pinholing and fishscaling defects in the enamel.

The above limitations of traditional enamelling derive from the need to heat both the enamel and the metal substrate to the fusion temperature of the enamel. Thermal spraying, particularly plasma spraying, has the potential advantage that the heat source is separated from the substrate. The coating powder is melted in the plasma and the temperature of the substrate can be maintained at a temperature as low as 100 °C if necessary. There is no furnace treatment and so, in principle, no restriction on component size. On-site enamelling of large components and on-site repair therefore become possibilities. Furthermore, the low substrate temperature is expected to eliminate pinholing and fishscaling in the enamel.

Thermal spraying refers to a family of processes in which a feedstock powder is injected into a hot jet where it is heated, accelerated and projected on to a substrate to form a coating. Individual processes include plasma spraying, high-velocity oxy-fuel spraying, combustion flame spraying and arc-wire spraying. In the current study, plasma spraying is investigated and a schematic of the process is given in Fig. 1. The high gas temperature (10 000–15 000K), velocity ($\sim$300 m s^{-1}) and heat content of the jet enable virtually any material to be melted and deposited, provided its melting temperature is below its decomposition temperature.[1,2] The process combines particle melting, cooling and compaction into a single process unlike conventional multi-stage enamelling.

The formation of the coating takes place in a number of steps. Heating and fusion of the feedstock particles in

* Corresponding author.
E-mail address: t.zhang@kingston.ac.uk (T. Zhang).

0955-2219/03/$ - see front matter
PII: S0955-2219(02)00235-2

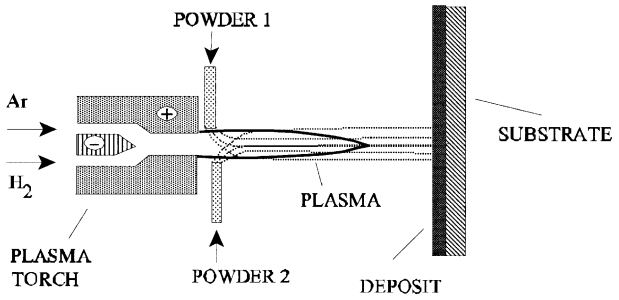

Fig. 1. Schematic of plasma spraying.

the hot jet, acceleration of the particles to a high velocity by the jet, impact and the flow of particle into a splat on the substrate surface. Finally, the splats accumulate and compact into a coating as a consequence of the scanning action of the spray gun. This sequence of events is shown schematically in Fig. 2. The residence time of a particle in the flame is less than one millisecond and so kinetics rather than thermodynamics dominate the mechanisms. Heat transfer from the plasma gas to the particle interior, the fluid mechanics of the jet flow and the rheology of the flow of the feedstock particles to form splats are important for the formation of dense, high-quality coatings.

The properties of the coating are governed by its microstructure, which depends on the process parameters and the composition of the material. In the particular case of enamels, these materials have high melt viscosities and so in order to achieve adequate flow of the splats on impact, the particles need to be accelerated to a sufficiently high velocity and heated to a high

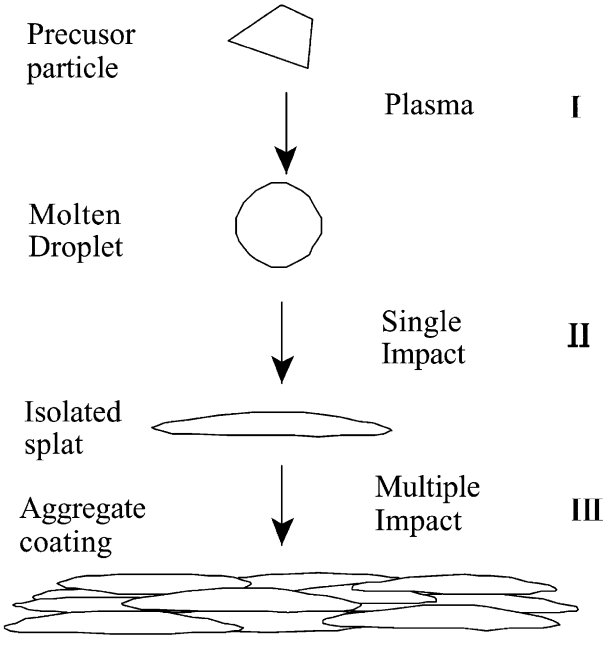

Fig. 2. Schematic showing stages of evolution of deposit during thermal spraying deposition.

enough temperature. In addition, the heating process is complicated by the relatively low thermal conductivity of enamel, which is expected to produce large temperature gradients in the particles during their flight from the gun to the substrate. An understanding of the process mechanisms is therefore essential for the development of a new enamelling technique based on thermal spraying. Theoretical modelling has in recent years given a better scientific understanding of the process and has increased coating performance. Several models have been presented in various papers for predicting coating thickness,[3–6] predicting plasma and in-flight particle temperatures,[7–11] and predicting deposit and substrate temperatures.[12,13] Nylen et al. have developed a computational model to simulate the temperatures on a gas turbine during plasma spraying. The results show that the temperatures on the surface of the coating vary between 800 and 950 K.[14] Lungscheider[15] and Mckelliget[16] have also developed a computational model to predict the temperature profile in the coating and substrate independently, but the results are very different from that obtained by Nylen et al. In these computational models, the temperatures in front of the substrate were taken from computational model and validated by experiments. However, the heat transfer coefficient was not discussed in these papers. In plasma deposition, the temperature profiles of the coating is controlled by the processing parameters such as arc power, compositions of the plasma gas, spray distances, scanning rate and the properties of the coating and substrates. To achieve desirable coating structures, it is necessary to understand the effect of these parameters.

This paper intends to present a simplified computational model for plasma-spray enamelling based on heat transfer and fluid mechanics. A computational model for an impinging jet was used to calculate the heat transfer coefficient between plasma jet and the substrate. The model simulates the process and computes the temperature profiles of the in-flight particles, the coating and the substrate during plasma spraying. The computed results are then compared with those from experimental trials. The research is aimed at investigating the feasibility of enamelling by thermal spraying and the effects of process parameters on the melting of in-flight particles and the temperature profiles of the substrate.

2. Experimental details

The coating material was a typical black acid-resistant frit with a softening temperature of 518 °C supplied by Escol Products Ltd (Huntingdon, UK), and milled and sieved to different sizes by Corus plc (Port Talbot, UK). The substrate material was aluminium-killed sheet steel of thickness 3 mm, supplied by Corus. The steel was degreased with acetone and surface roughened by grit

blasting (Metcolite C, alumina grit, Sulzer-Metco Ltd.) with a pressure-operated machine to give a surface roughness of 6 μm (R_a). Plasma spraying was undertaken using a Sulzer-Metco plasma spray system with an MBN torch and MCN control unit. A Sulzer-Metco 4MP powder feed unit and fluidized bed hopper was used to feed the powder into the plasma jet.

The temperature of the substrate during plasma spraying was monitored using thermocouples attached to the back of the steel substrate and the data was recorded on computer.

3. Computational model

3.1. The temperature of in-flight particles

A theoretical analysis has been carried out to predict the temperature profile of an enamel feedstock particle inside a plasma jet under various process parameters. To simplify the calculation the following assumptions have been made:

i The feedstock particle is spherical.
ii The particle is exposed to uniform atmospheric-pressure thermal plasma and the relative motion between the particle and plasma is neglected.
iii The temperature at the outside surface of the particles remains at below the thermal decomposition temperature; the change of radius due to thermal expansion was neglected.
iv The particle loading is sufficiently low for the temperature and flow fields in the plasma to be unaffected by the injected powder.
v Radiation from and to the particle is neglected.
vi To simplify the calculation, it is assumed that the particles travel along the axis of the flame.

The heat transfer within a spherical particle immersed in thermal plasma can be described by a special form of the general conduction equation in a spherical polar coordinate system:[17]

$$\rho C_{\mathrm{p}} \frac{\partial T}{\partial t} = \frac{1}{r^2}\frac{\partial}{\partial r}\left(kr^2 \frac{\partial T}{\partial r}\right) \tag{1}$$

where r is the radial distance from the centre of the particle ($0 < r < R$) as shown in Fig. 3. T is the temperature, t is the time, C_{p} is the specific heat and ρ is the density. The initial condition for solving this governing equation is:

$$T(r, t) = T_{\mathrm{c}} \quad \text{at } t = 0$$

where T_{c} is the carrier gas temperature.

An energy balance method was used for the calculation of temperature at the surface node s in which its internal energy change is equated to the heat transfer from the surrounding plasma and that from the adjacent internal node s-1 within the particle. This may be expressed as follows:

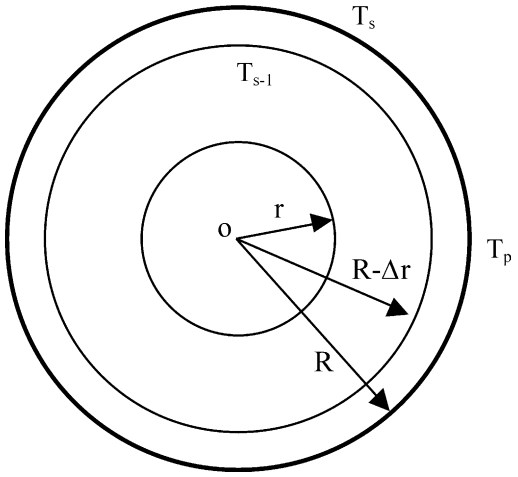

Fig. 3. Schematic of an in-flight paticle of radius R and a surface temperature T in a thermal plasma of temperature T, where r is the radial distance from the particle centre.

$$\left(1 - \frac{\Delta r}{R}\right)k(T_{s-1} - T_s) + h\Delta r\left(T_{\mathrm{p}} - T_s\right) = \frac{\Delta r^2}{2}\rho C\mathrm{p}\frac{\Delta T_s}{\Delta t} \tag{2}$$

where T_{p} represents the plasma temperature, which is a function of the axial and radial distance from the nozzle of the plasma gun. T_{s-1} is the temperature of the first internal node. h is the convective heat transfer coefficient between the plasma and the particle, which is dependent on the temperature and thermal conductivity of the plasma, and the surface temperature and size of the particle. The value of h was determined by the method given by Bourdin et al.,[18] which is now the widely accepted technique.[2,19–21] The integrated mean value of the thermal conductivity across the boundary layer, k, is given by the expression:

$$k = \frac{1}{\left(T_{\mathrm{p}} - T_s\right)}\int_{T_s}^{T_{\mathrm{p}}} k(T)\mathrm{d}T \tag{3}$$

which may be used for the heat transfer calculation under plasma conditions. The heat transfer coefficient is now given by:

$$h = \frac{1}{R\left(T_{\mathrm{p}} - T_s\right)}\int_{T_s}^{T_{\mathrm{p}}} k(T)\mathrm{d}T \tag{4}$$

where $k(T)$ is the thermal conductivity of the plasma gas at temperature T. It has been shown that Eqs. (3) and (4) can be used provided the residence time of the

particles in the plasma jet is longer than 1 μs.[18] This condition is readily satisfied in the current experiments and Eqs. (3) and (4) are used to calculate the heat transfer coefficient, h, of the plasma to the particles. Accordingly, a set of finite difference equations was written based on Eqs. (1) and (2) and used to obtain numerical solutions. Since the material investigated in this paper is glass, and the temperatures are below decomposition temperature, the fusion heat and decomposition enthalpies are not involved in the modelling.

3.2. Temperature profile of substrate and coating

A coating is formed by the repeated scanning of the substrate with a plasma torch as shown in Figs. 1 and 2. The horizontal distance between the nozzle exit and the vertical plane of the substrate is fixed throughout spraying, usually in the region of 100–130 mm. However, the distance between the intersection of central axis of the plasma jet with the substrate and any position P on the substrate surface must vary with the scanning action during spraying. This is shown schematically in Fig. 4.

The temperature and velocity of the flame or hot gas immediately in front of point P on the substrate are functions of scanning time as the torch moves across the substrate. This gas temperature governs the transfer of heat from the flame to the substrate and thus the resulting temperature of the coated component. The temperature of the component during spraying will exert a substantial effect on the product quality and so it is important that it is quantified.

In order to simulate the heating of a given point P on the substrate surface, the temperature profile and the heat transfer coefficient of the flame to the substrate must be pre-defined. Previous research work carried out by Tollmien[22] has indicated that the temperature of a jet may be described by a Gaussian distribution. However, this is only valid for a free jet and not one impinging on a substrate. Consequently, the authors have used a computational fluid dynamics (CFD) package to simulate the latter situation and determine the temperature

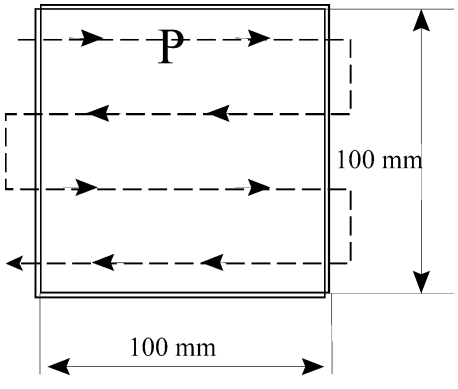

Fig. 4. Schematic of plasma scanning of the substrate.

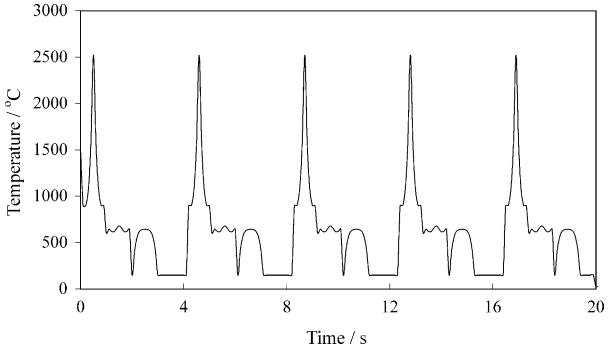

Fig. 5. The calculated plasma jet temperature immediately above a fixed point (P) on the substrate surface during plasma scanning.

distribution of the impinging jet. The computational method is explained in earlier papers by the authors.[23,24] The method is applied to the current case of a plasma jet and the results are given in Fig. 5. This predicts how the gas temperature in the plasma jet varies with the radial distance from the central axis.

Now that the temperature of the impinging jet has been calculated, the next step is to determine the heat transfer coefficient. Shimizu[25] has carried out experimental work to measure the heat transfer coefficient of a jet impinging on a plate. The measured data provide the heat transfer coefficient as a function of the radial distance from the axis of the jet. The experimental conditions are similar to those for a plasma jet impinging on the substrate and so the data was used in the present work.

The simulation is based on a 100×100 mm mild steel substrate with thickness of 1 mm. The thickness of the enamel coating is 0.2 mm. The flame axis is normal to the substrate and the spraying distance is 120 mm. It is assumed that there is a pre-deposited layer of glass coating of thickness 0.1 mm on the substrate. The plasma gas is taken to be argon with 5% hydrogen and the gas flow rate is 100 standard litres per minute.

To simplify the computation model, the following assumptions have been made:

i The heat transfer in the substrate is one-dimensional, since the thickness is much smaller than the width of the substrate (width/thickness = 100);
ii The scanning speed of the flame is fixed at 100 mm/s;
iii The vertical gap between each horizontal pass is 25 mm (The torch returns, therefore, to a given point after four passes as indicated in Fig. 4).
iv The presence of solid particles in the plasma jet was not considered in order to avoid the complication of their effect on the flame characteristics and coating thickness.

The temperature profile of the impinging flame immediately above a fixed point is a function of the size

of the substrate, scanning speed and the interval between each scan. Based on the assumptions above, the temperature above a fixed point (P) in Fig. 4 was calculated as a function of time during spring and presented in Fig. 5. In this particular case, it took 4 s and four passes of the torch to complete a full scan of the substrate. This process is then repeated to build up the coating thickness. It is noticed that the temperature change at point P is negligible in the last pass of each scanning cycle, since the centre of the flame is now far away from point P.

Based on these assumptions, the governing equation for the heat transfer in the coating and substrate can be expressed as:

$$\frac{\partial^2 T}{\partial z^2} = \frac{1}{D}\left(\frac{\partial T}{\partial t}\right) \tag{5}$$

where T is the temperature within the deposit or substrate at a distance z from the cold face of the substrate. The thermal diffusivities D are assumed to be constants for the substrate and coating respectively. At the boundary between the substrate and the coating, a combined element is considered. The heat transfer from the arc to the substrate can be written as:

$$q = h\left(T_{\mathrm{p}} - T_s\right) + q_{\mathrm{rad}} \tag{6}$$

where q is the total heat flux from the plasma jet to the substrate and h is the heat transfer coefficient. T_{p} and T_s are temperatures of plasma jet and the top surface of the coating respectively. q_{rad} is the radiative transfer from the plasma to the substrate. However, previous calculations by Nylen et al.[14] showed that q_{rad} can be neglected. Since the coating is an amorphous glass and the temperature is always lower than the melting point of the steel substrate, no latent heat changes were considered in the model.

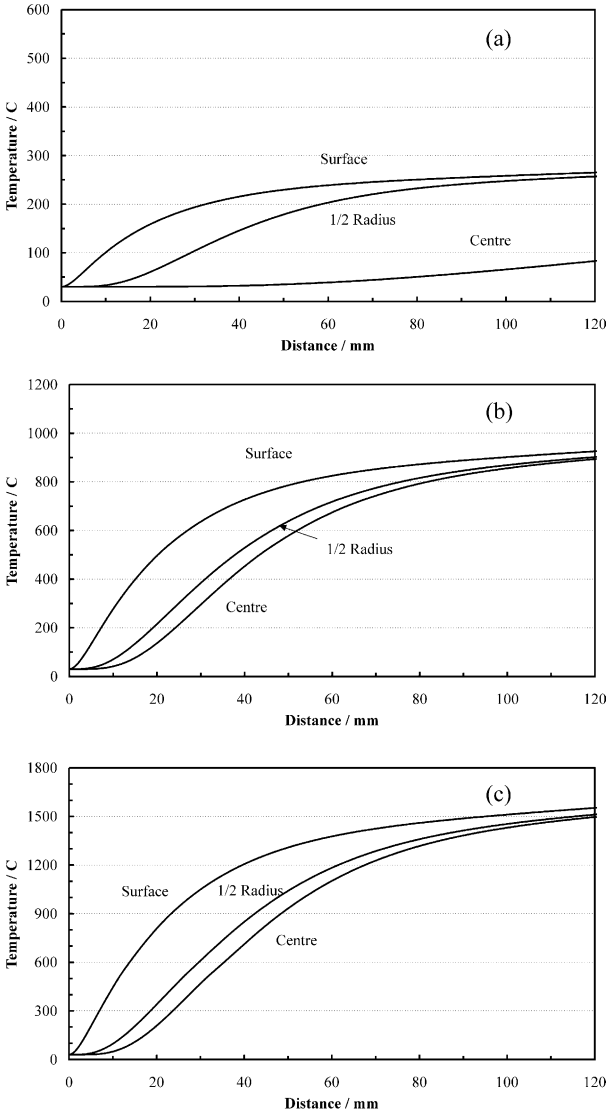

Fig. 6. Calculated temperatures of a 60 μm enamel particle at its surface, half radius and centre under different plasma conditions: (a) pure Ar, (b) 5% H_2–Ar, (c) 10% H_2–Ar.

4. Results and discussion

4.1. Effect of plasma flame on the heating of in-flight particles

The computational model described above was applied to the current case of enamel particles in a plasma jet. Initially, the effect of the hydrogen content on the heating of in-flight particles (diameter 60 μm) during plasma deposition was predicted using the model. The results are given in Fig. 6, which shows the predicted temperatures at the surface, half radius and centre of the enamel particle as it travels from its injection near the nozzle exit towards the substrate during spraying. Fig. 6a first gives the temperatures of a particle in a pure argon flame and shows a large temperature gradient from the surface to the centre of the particle. Furthermore, the temperature of the particle only reaches 270 and 90 °C at the surface and centre respectively. In physical terms, the particles remain in the solid state and rebound off the substrate on impact. As a result, deposition of an enamel coating using an argon flame is predicted to be impossible.

The addition of hydrogen to argon in the plasma gas is known to increase both the heat transfer coefficient and the gas temperature. Hydrogen contents of 5 and 10 vol.% were therefore added to the plasma gas and introduced into the computational model. The results are given in Fig. 6b for the 5% hydrogen–argon plasma and immediately show a dramatic increase in the particle temperature. The surface temperature of the particle now reaches 900 °C as compared with 270 °C in the

pure argon plasma. The temperature gradient within a particle is important, since it is necessary to obtain melting throughout the thickness not only at the surface. At short distances from the nozzle exit, the temperature gradient between the surface and centre of the particle is large and reaches 400 °C at a distance of 30 mm. However, the gradient gradually reduces and is only 40 °C at 120 mm, which is approximately the spraying distance. This means that the particle has a virtually uniform temperature by the time it impacts with the substrate. The reason for this equalization of temperature is because the temperature of the plasma flame falls rapidly along the axis of the flame: from approximately 10 000 °C at near the nozzle exit down to 2500 °C at 120 mm along the central axis. This lessens the heat transfer from the gas to the particle surface, while the rate of internal conduction from the surface to the centre of the particle remains high.

The effect of adding 10% hydrogen to argon was also computed using the model and the results given in Fig. 6c. The temperature of the particle surface now reaches 1500 °C with its centre being only 40 °C lower. These temperatures are so high that they may possibly cause degradation of the enamel.

Experimental trials were carried out to test the above predictions. It was found that no coatings could be produced with a pure argon plasma whereas coatings were formed using a 5% hydrogen–argon mixture. This behaviour is in agreement with the computational model. However, the 10% hydrogen–argon plasma produced dense enamel coatings with no evidence of thermal decomposition. This is surprising in view of the known decomposition characteristics of enamel. It is likely that this is a consequence of the extremely rapid kinetics of plasma spray deposition rather than a limitation of the model. The velocity of an enamel particle entrained in the high-speed plasma jet will be 100–200 m/s over a spraying distance of 100 mm, which gives a residence time of less than 1 ms. The results indicate that decomposition of the enamel does not take place, possibly due to the extremely short time period. The residence time of particles in the flame is less than 1 ms. Therefore, the time for the particles remains at temperature above the decomposition temperature will be less than 0.5 ms. This means that the enamel can exist at much higher temperatures than under equilibrium conditions and this can bring benefits to the coating quality. In order to form a dense coating, the impacting particle has to flow extensively into a thin splat in less than a millisecond as illustrated in Fig. 2. Enamels, like most other glasses, have inherently high viscosities and the abnormally high temperatures achievable in plasma spraying facilitate large-scale viscous flow, which enables the formation of dense coatings.

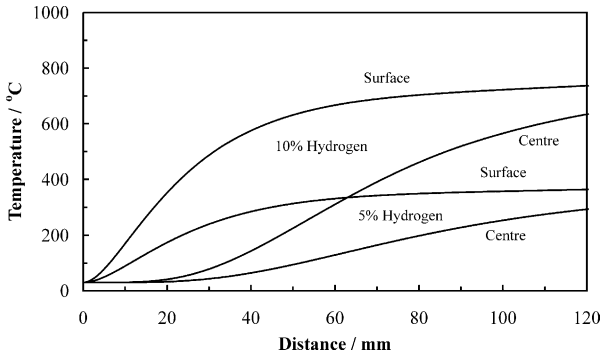

Fig. 7. Calculated temperatures of a 90 μm enamel particle at the surface and centre at various plasma conditions.

4.2. The effect of particle size on the heating of in-flight particles

The model was applied to calculate the effect of the particle diameter on the temperature of in-flight particles. Fig. 7 gives the temperature profile of a 90 μm particle in a 5% hydrogen–argon plasma and a 10% hydrogen–argon plasma. The results show that in a 5% hydrogen flame, the particle only reached a maximum of 370 °C at its surface and so is predicted to remain in the solid state. With 10% hydrogen, the results in Fig. 7 show that the heating is expected to be much improved as the surface and centre of the particle are raised above 630 °C.

Trials were then undertaken with 90 μm ($D_{50} = 90$ μm) particles but this time using a 10% hydrogen–argon plasma. Fig. 8a gives the microstructure of a through-thickness cross-section of the coating deposited under these conditions. The coating is porous and of low quality owing to insufficient flow of the particles on impact. Referring back to Fig. 7, it is seen that the temperature is barely above the enamel fusion temperature and that substantial temperature gradients remain between the surface and centre of the enamel particle.

Further spray trials were carried out with the 10% hydrogen–argon plasma but now using much finer feedstock powder: D_{50} of 57 μm. The microstructure of the resulting coating is given in Fig. 8b. This shows a high-quality, dense coating of enamel. The corresponding computational data are given in Fig. 6b. The implication from these results is that high particle temperatures and velocities together with fine feedstock powders are required to deposit sound enamel coatings under the conditions used.

4.3. The temperature profile of coatings during deposition

The temperatures in the coating and substrate during plasma scanning were computed using the model in previous section and the results are presented in Fig. 9. This gives the temperature at the top surface of the coating, the interface and the back of the substrate. The temperature of the surface of the coating is predicted to

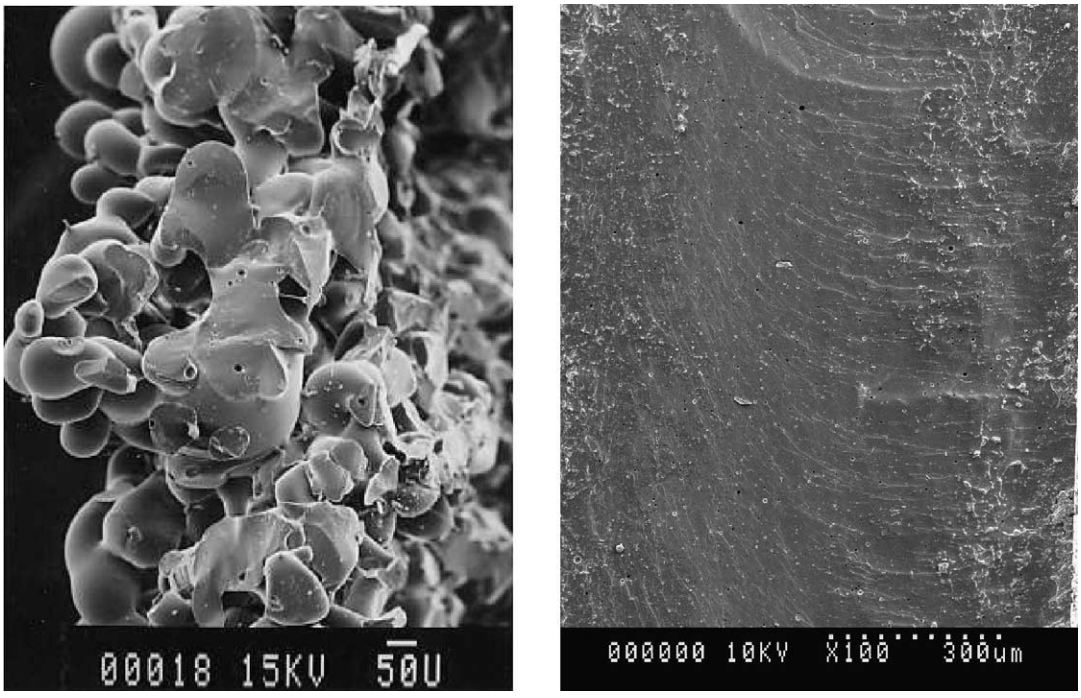

Fig. 8. Cross-sections of coatings deposited using feedstock particles of diameter: (a) 90 μm, (b) 60 μm.

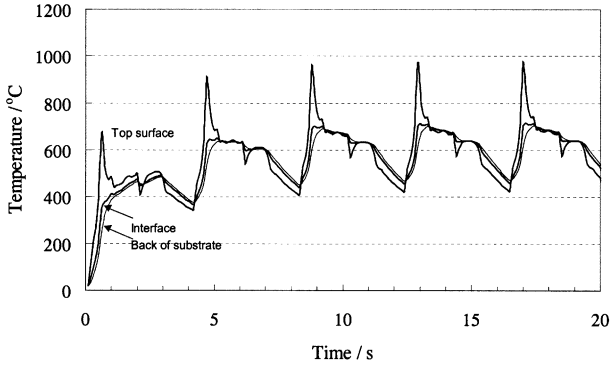

Fig. 9. The temperature distribution in the coating and substrate.

increase very rapidly in the first second, since the point P (Fig. 4) is close to the centre of the flame and the gas temperature and heat transfer coefficient are both very high. The temperature in the substrate increases much more slowly. Although the thickness of the substrate is 5 times the thickness of the coating, the temperature gradient in the coating is still much higher than that in the substrate. This is caused by the fact that the heat transfer at this stage is controlled by conduction and the thermal conductivity of the steel substrate is much higher than that of the enamel.

At the fourth second, the temperature in the front of the coating is lower than that at the back of the substrate. This is because the gas temperature of the coating surface at P is lower than that at the substrate and furthermore, the heat transfer coefficient is higher at the coating surface than that at the back of the substrate due to much higher gas velocity. As scanning continues, the temperature difference between coating and the plasma gas at P is smaller and the rate of temperature rise becomes slower. After four complete scans, there is no significant change between the coating and substrate temperatures and thermal equilibrium is reached. These results from the computational model show that during each plasma scan, the plasma torch produces a high thermal shock to the front surface of the coating and this generates a high temperature gradient in the coating. The effect is particularly marked for low-conductivity coating materials such as enamels. In order to test the computer predictions, thermocouples were welded to the back of the steel substrate. The temperatures measured during spraying were found to be similar to and follow the same trends as those in the model.

The work in this paper focuses on how the temperature profiles depend on the plasma gas composition and the feedstock particle size. However, other process parameters will also have an influence. For instance, the model also shows how the temperature in the coating depends on the scanning method and the component size. If the interval between each scan is extended or the area of the substrate is increased, the computations indicate that the temperatures of the coating and substrate will reduce by a substantial amount.

5. Conclusions

- Computer models have been developed to simulate the temperature profiles of feedstock particles

during their flight in the plasma and those of the coating and substrate during spraying.

- The computational model for the in-flight particles shows that a process window for the formation of dense enamel coatings can be determined in terms of the plasma gas composition and the particle size.
- The model for the heating of the enamel coating and substrate during scanning indicates that the plasma jet produces a thermal shock at the surface of the coating and a high temperature gradient through its thickness.
- Experimental spraying trials confirmed the computational model and dense coatings were successfully produced.

Acknowledgements

The research was sponsored by the Engineering and Physical Sciences Research Council and the UK Department of Trade and Industry and carried out in collaboration with Corus plc and Escol Products Ltd under the LINK Programme in Surface Engineering. The authors would like to thank the above for their support.

References

1. McPherson, R., *Thin Solid Films*, 1981, **83**, 297–310.
2. Vardelle, M., Vardelle, A., Fauchais, P. and Boulous, M. I., *AICHE i.*, 1983, **29**, 236–243.
3. Goedjen, G., Miller, R. & Brindley, W., *A Simulation Technique for Predicting Thickness of Thermal Sprayed Coatings*. NASA Army Research Laboratory Technical Report ARL-TR-762, 1995.
4. Mikosch, F., Precise Manufacturing with Off-line Programmed Robots Integration in Manufacturing Enables Innovative Robotics Solutions. ESPRIT Project No 6457, 1995, 331–340.
5. Cirolino, S., Harding, J. H. and Jacucci, G., Computer simulation of plasma-sprayed coatings I. Coating deposition model. *Surface and Coatings Technology*, 1991, **48**, 137–145.
6. Fasching, M. F., Prinz, F. B. and Weiss, L. E., Planning robotic trajectories for thermal spray shape deposition. *Journal of Thermal Spray Technology*, 1993, **2**, 45–50.
7. Szekely, J. and Westhoff, R.C., Recent advances in the mathematical modelling of transport phenomena in plasma systems. Thermal Plasma Applications in Materials and Metallurgical Processing, 1992, pp. 55–72.
8. Chang, C. H., Numerical simulation of alumina spraying in argon–helium plasma jet, of thermal spray. In *International Advances in Coatings Technology*, ed. C. C. Berndt. Pub. ASM International, Materials Park, OH, 1992, pp. 793–798.
9. Vardelle, M., Vardelle, A., Fauchais, P. and Boulos, M., Plasma-particle momentum and heat transfer: modelling and measurements. *AIChE Journal*, 1983, **29**(2), 236–243.
10. Pfender, E., Particle behaviour in thermal plasmas. *Plasma Chemistry and Plasma Processing*, 1989, **9**(1), 167–195.
11. Pfender, E. and Lee, Y. C., particle dynamics and Particle heat and mass transfer in thermal plasmas. Part I. The motion of a single particle without thermal effects. *Plasma Chemistry and Processing*, 1985, **5**(3), 211–237.
12. Knotek, O., Balting, U., Cosack, T. and Pantucek, P., Measurements and mathematical modelling of heat flow into substrates during atmospheric plasma spraying of coated compounds as a starting point for strain calculations. *2nd Plasma Technik Symposium*, 1991, **1**, 103–110.
13. Leyers, H., Adamietz, H., Sbuchkremer, H. and Stover, D., Heat transport between plasma jet and workpiece in plasma spraying. *2nd Plasma Technique Symposium*, 1991, **1**, 111–121.
14. Nylen, P., Wigren, J., Pejryd, I. and Hansson, M., Modelling of coating thickness, heat transfer and fluid flow and it's correlation with the TBC microstructure for a plasma sprayed gas turbine application. In *Thermal Spray: Meeting the Challenges of the 21st Century,* Vol. 1, ed. C. Coddet. ASM, OH, USA, 1998, pp. 361–366.
15. Lugscheider, E., Barimani, C., Eritt, U. and Kuzmenkov, A., Fe-simulations of temperature and stress field distribution in thermally sprayed coatings due to deposition process. In *Thermal Spray: Meeting the Challenges of the 21st Century,* Vol. 1, ed. C. Coddet. ASM, OH, USA, 1998, pp. 367–372.
16. Mckelliget, J. W., Trapaga, G., Gutierrez-Miravete, E. and Cybulski, M., An integrated mathematical model of the plasma spraying process. In *Thermal Spray: Meeting the Challenges of the 21st Century,* Vol. 1, ed. C. Coddet. ASM, OH, USA, 1998, pp. 335–340.
17. Croft, D. R. and Lilley, D. G., *Heat Transfer Calculations Using Finite Difference Equations*. Applied Science Publishers Ltd., London, 1977 pp. 1–87.
18. Bourdin, E., Fauchais, P. and Boulos, M., *Int. J. Heat Mass Transfer*, 1983, **26**, 567–582.
19. Bonet, C., *Pure Appl. Chem*., 1980, **52**, 1707–1714.
20. Chen, X. and Pfender, E., *Plasma Chemistry and Plasma Process*, 1982, **2**, 185–212.
21. Joshi, S. V. and Sivakumar, R., *Mater. Sci. Technol*., 1992, **8**, 481–488.
22. Tollmien, W. *Berchnung turbulenter ausbreitungvorgange*, NACA TM, 1085–1945.
23. Bao, Y., Zhang, T. and Gawne, D. T., Analysis of residual stress generated during plasma spraying of glass coatings. In *Thermal Spray: Meeting the Challenges of the 21st Century, Vol. 1*, ed. C. Coddet. ASM International, OH, USA, 1998, pp. 575–580.
24. Zhang, T., Liu, B., Gawne, D. T. and Bao, Y., Computer simulation of shrouding on the profile of a plasma jet. In *Thermal Spray 2001: New Surface for a New milennium*, ed. C. Berndt, K. A. Khor and E. F. Lugscheider. ASM International, OH, USA, 2001, pp. 895–902.
25. Shimizu, A., Impinging jet heat transfer with gaseous-solid suspension medium. *Advances in Enhanced Heat Transfer, Symposium volume of the 18th National Heat Transfer Conference*, San Diego, 1979, pp. 155–160.